

Microwave and Millimeter-Wave Systems: Propagation Studies at 5G Wireless Bands

Lizette Rodriguez, Emiliano Novas, Angela Speck¹, Rafael Rodriguez², Rafael Medina²

^a*University of Texas at San Antonio¹, 1 UTSA Circle, San Antonio, 78249, Texas, United States*

^b*University of Puerto Rico at Mayagüez², 9000 University of Puerto Rico at Mayagüez Calle Post, Mayagüez, 00681, Puerto Rico, United States*

Abstract

5G technology has made wireless communication effortless, along with these advancements researchers have accrued knowledge in what makes 5G technology reliable and how its properties can further progress research in electronics and astronomy alike. During the summer of 2023 two researchers went into the lab and field and conducted three phases of research to understand properties of signals and their behavior, most specifically path loss and interference. Along the span of the summer researchers conducted research across three different environments (or phases) each containing different attributes or characteristics that appealed to researchers. Some of the following qualities that appealed to the researchers when choosing settings to take infield and in-lab data from include temperature change, topographic change, and accessibility. Being able to accurately measure and predict the effects of path loss and interference came purposefully when choosing settings and allowed for a more accurate use of data analysis within the 2-month research stent at the University of Puerto Rico at Mayagüez. The tabulated data and models below translate the direct effects of interference on a multitude of instruments used in the summer research stent: signal generators, spectrum analyzers, Gain Horn antennas, HyperLog® antennas and many other instruments across all three phases of research. This data proves instrumental in optimizing 5G signals because of the path loss research done in millimeter wave and microwave 5G band systems. It was found that the effects of path loss are more severe on higher frequencies, while lower frequencies tend to undergo more interference. Plans include measuring the radiation patterns of transmitting antennas at 5G bands in an an-echoic chamber using a vector network analyzer, and to develop a fully integrated user-friendly GUI that can help automate and expedite the process to accomplish said task.

Keywords: Path Loss, Interference, Radiation Patterns, 5G Technology

1. Introduction

This project's focal point is path loss and interference in 5G bands. To lay the foundation for the project, the behavior of signals at 5G bands was observed when subjected to conditions where the signals undergo path loss due to environmental factors, such as wind, humidity, rain, angle and lateral displacement of the signal source/transmitter with respect to the signal receptor, physical obstacles in between the transmitter and receptor, and when subjected to interference at nearing and equal frequencies from other signals. The goal is to find a way to mitigate said factors, such that the transmitted signal can be sent and received more efficiently, with less path loss, and lower adverse effects due to noise and direct interference. [1][2]

2. Background

2.1. 5G Technology

The term 5G refers to the fifth generation of mobile wireless communications technology. 5G signals are transmitted in millimeter-wave and microwave bands, which are at frequencies above 1GHz. For this project, four frequencies were investigated, those being 1.9GHz, 3.7GHz, 28GHz, and 39GHz. 1.9GHz and 3.7GHz would be classified as microwave bands, while 28GHz and 39GHz are millimeter-wave bands. Lower

frequencies tend to provide better coverage due to the longer wavelength, which results in less path loss, while higher frequencies provide higher speeds but less coverage.[2]

2.2. Friis Equation

The Friis equation describes the expected received power of a signal transmitter under the conditions that both the transmitting and receiving antennas are isotropic and in free space:

$$P_r = \frac{P_t G_t G_r \lambda^2}{(4\pi R)^2} \quad (1)$$

For the path loss experiment, the signals were propagated at the following frequencies: 1.9GHz, 3.7GHz, 28GHz, and 39GHz. Said frequencies are rather high, which would actually serve to decrease the received power due to the smaller wavelength. Said decreased theoretical power was reflected when the task to find the 1dB compression points was undertaken, which will be discussed in more detail in the methodology.

2.3. Interference

Interference/noise is another important factor to consider for the transmission and reception of a signal. Signal interference is defined as when a signal is disrupted or weakened due to the presence of other wireless signals. This can be manifested as static, which can muddy the signal and appear as background

noise, or if severe enough, can completely blot out the signal that is supposed to be measured and studied. Another thing to consider when dealing with interference is the noise floor. The noise floor can be seen as the amalgamation of every other signal being transmitted at the same frequency that could interfere with your signal, but is either too far or not potent enough to cause significant disruption. When observing the signal spectrum, the noise floor manifests itself as a horizontal line with several small oscillating peaks at a relatively constant power, however that power depends on the time of day due to the difference in levels of activity on whatever band that is being measured in, and it also depends on the actual band itself. For example, the noise floor at 2.4 GHz is approximately -105dBm, and the noise floor at 5GHz, which is a much more commonly used band for wireless signals, is about -95dBm, which is ten times higher than the noise floor at 2.4GHz. [2]

During the interference part of the project, an oscillator was used to artificially generate interference. On the frequency spectrum, we could graphically see the signal received from the radio vs the oscillator. The oscillator generates an electrical signal with a peak, and something called a skirt, at its base. Ideally, the signal from the oscillator should solely be observed at the frequency it's tuned to, however, at the signals base, there is a triangle shaped area with the peak placed at the center, and a band of frequencies adjacent to the peak that are receiving part of the signal. This area is called the skirt, and its bandwidth is called the skirt width.

2.4. Antenna Radiation Patterns

An antenna radiation pattern is a graphical way of representing an antenna's radiation properties using space coordinates. The most important property observed in an antenna's radiation pattern is the spatial distribution of radiated energy with respect to the observer's position. Figure 1 represents the radiation pattern for the transmitting (left) and receiving (right) standard gain horn antennas at 28GHz and 39GHz. The following equations describe the span of the antenna under test, with D being the antenna diameter, P being the probe diameter, Z_p being the distance between the antenna under test and the probe, and theta being the maximum processing angle from bore-sight.[3]

$$a = D_x + P + 2z_p \tan(\theta) \quad (2)$$

$$b = D_y + P + 2z_p \tan(\theta) \quad (3)$$

2.5. 1 dB Compression Point

When computing the theoretical input power vs output power of an amplifier on a graph, it looks like a straight line with a defined slope. In practice, however, amplifiers have a saturation point, at which no matter how much the input power is increased, the output power will not change with respect to the previous input.[2] There is a point on that graph where the line curves, and the gain from the amplifier is 1 dB lower than the calculated gain. That is the 1 dB compression point, and it serves as the point in which the maximum feasible power is drawn from the amplifier without saturating it. For this project,

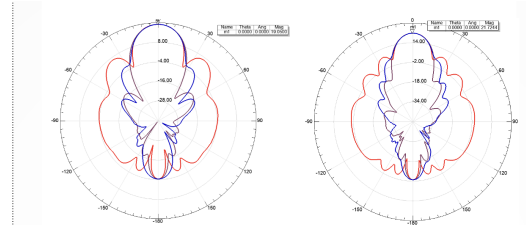


Fig. 2: Type Horn Antenna 22240 at 28 GHz

Fig. 3: Type Horn Antenna 22240 at 39 GHz

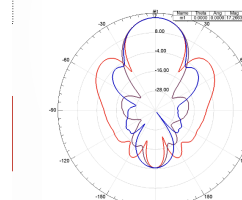


Fig. 4: Type Horn Antenna 23240 at 28 GHz

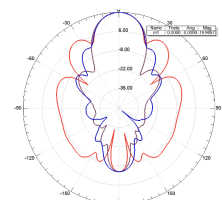


Fig. 5: Type Horn Antenna 23240 at 39 GHz

— dB (Total Gain) at Phi = 0° degrees
--- dB (Total Gain) at Phi = 45° degrees
— dB (Total Gain) at Phi = 90° degrees

Figure 1: Horn antenna radiation patterns at 28GHz and 39GHz.

four 1 dB compression points were needed on account of the four frequencies being tested at. Each frequency has a different wavelength, which affects the power received by the amplifier, it being lower on the higher frequencies, and higher on the lower frequencies.

3. Methodology

3.1. 1dB Compression Analysis (Phase 1)

During the preliminary days of in-field testing, a signal generator was used to transmit signals at frequencies 1.9GHz, 3.7GHz, 28GHz, and 39 GHz. Using a spectrum analyzer, the researchers took note of power levels coinciding with INT (integer) values provided by the spectrum analyzer. The bounds of INT values tested for all 4 frequencies range from -20 to 6. During data collection a series of power outputs were put into a table via LabPlot where the researcher generated graphs that later became the basis for the points of what is called: 1dB decompression points. This point is the point before the signal saturates the spectrum analyzer and it is ineffective to take note of the INT value because of the signal loss caused by increasing INT values. From this data the researchers found individual INT values that best made for efficient data across the in-field testing of Gain horn antennas, omni-directional whip antennas and HyperLog® antennas each with different capacities and different in and out field characteristics.

3.2. Linear Analysis or Point to Point Antenna Set-up (PTP)

The First in-field testing environment is a hallway with minimal airway exposure with as seen in Figure 2 above. The carts



Figure 2: Linear Set-up of a Signal Generator, Spectrum Analyzer, Windows PC, and Transmitting /Receiving Gain Horn Antennas in Red Carts at UPRM (ENV 1)

lay horizontally 10 ft across the signal generators point of origination. Further down the hallway the walls tighten with the measured length across being 6ft. To the left of the carts lies a space of 21 inches that consistently was needed to reference point of origins within the in-field experiments taken place. This minimal airway exposure hallway will serve as environment one or (ENV 1).

As mentioned, the signal generators position lies at the point of origination which describes the stationary position where the cart is denoted as the transmitting signal in reference to the connected Gain Horn 22240 Antenna on top of the carts point of origination. Directly linear to the point of origination at a displacement of 0.3048 meters is the receiving Gain Horn 22240 antennas beside it in the set up lies the portable spectrum analyzer and windows PC. This all used to experiment with propagation loss at frequencies 28GHz and 39GHz.

PTP data collection was accomplished by denoting the environments humidity and temperature levels. After a brief note was taken of the environment's temperature and humidity using a portable Kestrel thermostat the researchers would stand one each at the receiving and transmitting ends of the signals path loss. During this state of data accumulation one researcher would stand at the point of origination and correctly align the Gain Horn 22240 antenna to the receiving end and set the signal generators settings to either 28GHz or 39GHz along with the appropriate calculated 1db compression point calculated in the step before this discussion. After the INT value was placed in the settings of the signal generator the researcher in the receiving end of the propagation loss signal would make sure the spectrum analyzer was connected to the PC. Furthermore, the researcher would have to make sure the wire to the spectrum analyzer was screwed on to the device and the antenna sufficiently for data collection.

During the data collection phase, the researcher on the re-

ceiving end would look at the ANSYS® software and select the appropriate integer values in the side tool bar for bandwidth, frequency, and peak markers. These setting values consisted of a frequency in values or either 28 or 39. Option values such as Bandwidth were always consistently placed in the value of 4. Peak markers (usually the last setting option selected during data collection) are used to help determine a consistent power output during the data collection phase.

The researchers would change the setting values between the various noted frequencies above and then would in this stage of the data collection phase get incrementally farther and farther away from the point of origination. Collecting peak values at various distances allowed both researchers to compile the data across both frequencies in terms of the output power that was received at different points. In this case for the PTP analysis the incremented values of 0.6096 m then at 3.048 m the increments decrease to 0.3048 m.

3.3. Point to Point Lateral Analysis (PTPL)

After discovering that the propagating signal had yielded consistent power signals at the end of the tested linear distance, using the same ENV 1 and equipment researchers in the same fashion used the same proceeding notions of the PTP Analysis to analyze lateral displacement to understand signal loss in the negative direction.

Following the sequence of events of the last in-field experimental set-up researchers first measure humanity and temperature levels of the air as denoted by figure 2 bellow. To test propagation signal loss on a lateral level the researchers used the incorporation set-up of PTP set-up that the researchers use previously. This accomplished the analyzation of whether researchers could account for similarly PTP results within the second trial of in-field testing of propagated signal loss in ENV 1. Incrementally the researchers distanced themselves from the point of origination, but also after accounting for the output powers values at those increments would step in negative increments to the side of indirect signal source to analyze the different data points of signal loss.

In this in-field experiment data was obtained in different PTP distances. The receiving Gain horn antenna end obtained data at the 3.048 m mark. From this distance linear increments of 3.048 were implemented to best measure path signal loss. At the 18.288 m mark increments of 6.096 were implemented since the PTPL analysis had considerably shown that within this period that the signal generator at both frequencies compressions points had not reached the signal threshold generated on the ANSYS® software. At every incremental PTP distance mark a negative displacement increments of 0.3048, 0.6096, 0.9144 meters was taken to measure the power output peaks. This was to theoretically measure the PTPL distance of the signal threshold of the signal generator.

3.4. Point to Point Angular Analysis (PTPA)

After consistent trials in lateral and linear data the researchers changed the environment to environment 2 or (ENV2) with moderate hallway exposure. The carts lay 1.143 m apart as

seen in the figure above. In the context of the trials with in-field data a HyperLog® antenna was used instead of a Gain Horn antenna because of the HyperLog's® omnidirectional antenna properties that allow for better angular change in in-field signal loss testing in ENV2.

As mentioned in previous trials the signal generator lies at the point of origination. The only thing different about the set-up for the angular analysis is the HyperLog's® position (this being at the point of origination were the transmitting gain horn antenna used to be). On the receiving end is the OmniLOG39000®, is an omnidirectional receiver and is the counterpart to the HyperLog ®. Other than the replacement of the Grain horn antennas the equipment such as the carts used to wheel the spectrum analyzer, signal generator, the windows laptop, and the ANSYS® software remain the same.

PTPA data collection was accomplished similarly to the last in-field trial in ENV1. Similarly, the researchers measured out an appropriate increment to first test linear signal threshold and then tested parameters of signal in lateral and angular propagation signal loss. ENV 2 allowed for the researchers to go farther than EVN 1 and upon doing so the measurements of linear and lateral displacement changed upon moving the receiving end of the HyperLog® antenna. In linear displacement increments of 2.286 m were implemented until the value 43.434 m. After that measurement of displacement 1.7399 m was used to cover more ground towards the end of the hallway in ENV2. Laterally the displacement changed due to the although lengthier environment was narrower then ENV1, so instead of the negative increments as listed in the last trial the researchers were only able to environmentally accomplish 0.3048 and 0.6096 m in the negative direction. As instructed in the previous trials the sets of data were taken in the same exact manor as in the linear and lateral trials with both researchers on opposite ends of each other while the researcher on the receiving end displaced the red cart incrementally as instructed linearly, laterally, and angularly every 2.286 meters or so.

Angularly the researcher that was transmitting would use a protractor and align the protractor horizontally and vertically with the HyperLog®. this would then allow the researcher to tilt the antenna to the desired angular displacement in both positive and negative directions. In the case of this in-field testing increments of 30° and 90° were best desired to test the propagation of signal loss in both positive and negative directions alike.

3.5. Software-defined Radio Studies (SDR) (Phase 2)

Using the Software-defined Radio software researcher able to use an omnidirectional whip antenna to conduct a series of observational studies in the lab to discover properties of the effects that purposeful interference cause to the signals and center frequencies across multiple FM and AM stations.

After the installation of the SDR software the researchers were able to use a spectrum analyzer, signal generator, and omnidirectional whip antenna to review transmitted radio signals across multiple frequencies. The spectrum analyzer had multiple ports in the set-up for the in-lab testing two of the four ports were used in the in-lab set-up. This set-up was made so that

Omni-Antenna Purposeful Interference Data

<i>Amp(dBm)</i>	<i>Skirtwidth [kHz]</i>	<i>CenterFreq(mHz) [Start and Stop]</i>
-30	-70	-90.2, 90.42
-27	78	90.15, 90.45
-24	88	90.2, 90.48
-21	100	90.05, 90.65
-18	108	90.03, 91.54
-15	140	89.4, 91.17

Table 1: The Omni-Antenna Interference data that describes the characteristics of the interference curve over FM stations in the higher frequencies

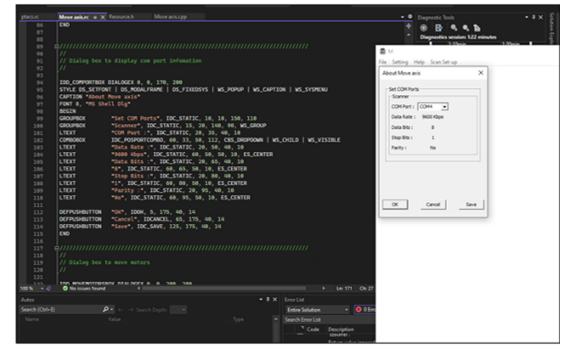


Figure 3: This figure is a picture of the Markdown interface used to generate the white window to the right which is used to communicate to VXM motors which motors to move at which fixed rate

the spectrum analyzer would connect to the windows PC and the signal generator that was used to interfere with the SDR alongside the omnidirectional whip antenna.

During the study a list of observations were compiled in a table via excel to analyze the effects of the interference on the radio station 90.2. In this figure things like the magnitude (amplitude), skirt width, and center frequency were taken note of during the SDR in-lab study. Characteristics such as: "center frequency" and "start and stop" denote the interference frequency points at which the interfere starts and stops are denoted above in the figure above. Skirt width in the table above defines how wide the interference mark was in the SDR software. All these characteristics within the study characterize behavior of what was seen while moving the frequency and amplitude dials on the signal generator to purposely generate interference within a Software-defined Radio studies phase.

3.6. Graphical User Interphase for Radiative Prints (GUI) (Phase 3)

After both in-lab and in-field experiments were conducted a series of theoretical studies was conducted to reenforce the

theoretical radiative prints of antenna sets used in-lab studies and in-field studies alike.

This in-lab set up consisted of an anechoic chamber that was covered in pyramidal microwave absorbing foam with specifically allowed the anechoic chamber to provide exact radiative prints for the reoccurring process above. In the anechoic chamber two parts of the radiative machine work together to provide the basic radiative prints for antennas for in-lab testing. The bi-slide system refers to the frame of the machine in collation with the arms that work together with counterpart servo motors or VXM motors to systematically sweep a certain number of steps per second within the machines allotted period. Directly outside of the anechoic chamber is where both researchers coded a user-friendly GUI in a windows PC to accurately move and interpret physical movements/commands made by the VXM motors and bi-slide system.

The Bi-slide system is an arc frame that must be perfectly aligned with its counterpart directly across from it. To accomplish this both researchers used a serve of screwdrivers and Allen wrenches to unscrew items pf the Bi-slide system that were not properly aligned about measurements cucleated previously. Some of the items used to measure the distance includes a micrometer, ground leveler, and a caliper. after all the readings were leveled and conclusively stated that the bi-slide bars were equidistant to each other a series of test runs including the COSMOS® software was used to test the bas functionality of the VXM motors along with the Bi-slide arms. The series of tests ran allowed both researchers to further calibrate and take note of things such as the velocity that must be set for the VXM motors to move and the steps per second that can experimentally and theoretically be accomplished in a certain period.

Taking note of observations made in the set up and alignment of the machine allowed both researchers to accurately curate a GUI a system using Microsoft's® Visual Studios (2022). The software program provided the basic layout to the GUI seen in figure 3 below. Three separate files were created¹ in the creation of the "Move axis" project title.[4] The first file was a markdown of what the files interface is set to looked like as seen in the same figure as mentioned. The second file is a file that was used was a .h file that served as a file that defined basic outlining variables for the .rc file and .cpp file (the markdown and C coded files). The third file used was the coded C file were both researchers used recourses such as the VXM user manual to encode movements that the VXM motors and the Bi-slide system could recognize to easily interpret data faster for future uses. These sets of movements were connected to the GUI user interface that was designed by both researchers during the preliminary makings of the graphical interphase. [5][6]

4. Discussion

4.1. Path Loss

The conditions for the path loss experiment were not as described in the Friis equation. The path loss experiment was

conducted in a relatively narrow hallway, which could actually enhance the signal being received. While there were physical obstacles between the transmitting and receiving antennas, like columns and, at times, people, part of the transmitted signal that would otherwise be lost in free space, could potentially be reflected off the walls, and that reflected signal could reach the receiving antenna, which would result in a higher power signature. This is appears to be the case, since upon using the Friis equation to calculate received power for the different inputs, and comparing it to the actual data that was taken, at the farther distances the power that was measured at the receiving antenna was orders of magnitude higher than the calculated theoretical value.

Despite being higher than expected, the received power displayed the expected behavior given the experiment conditions. First and foremost is the measured received power at increasing linear distances. As the distance between the transmitting and receiving gain horn antennas increased, the received power measured at the spectrometer displayed a logarithmic decreasing pattern. The farther the receiving antenna, the slower the decrease, and the closer the signal came to the noise floor. The noise floor itself wasn't reached due to the constraint of the length of the hallways, however, on the higher distances the signal waned more and more slowly, as was expected.

For the lateral displacement part of the path loss experiment, we hypothesized that at the distances that were closer to the transmitting antenna, the gain loss upon lateral displacement would be much more severe when compared to the greater distances. Upon experimentation, the results were in line with the hypothesis. In the shorter distances, due to the physical characteristics of the radiation field of the transmitting antennas, when the receiving antennas were laterally displaced, it was as if they were being almost completely removed from that field. This results in a much weaker received signal, which is reflected in the results.

For the angular displacement, the environmental conditions of the experiment are of paramount importance to consider when analyzing the results. In this project's case, the equipment included the standard signal generator and spectrometer, but the transmitting antenna was a very directional antenna, namely the HyperLog®6080, and an omni-directional receiving antenna; the OmniLog®30800. This is an important detail when taking into consideration the signal's physical reflective properties, and its effects are clearly seen in the results. The direction to the left of the transmitting antenna was denoted as negative, and the direction to the right was denoted as positive. Since to the right of the antenna there was a wall, and to the left there was essentially free space, the signal power received when subjecting the transmitting antenna to angular displacement in the positive direction was significantly higher relative to the power received with negative angular displacement.

4.2. Interference

For the radio frequency part of the project, we were able to observe the peak of the signal from the oscillator and were able to hear the static and interference as the oscillator's power was increased and as the oscillator's frequency was tuned so that it

¹Project Page: UPRM Github, 2023, Rodriguez, Novas

Hyperlog® PTPLA Data at 3.7 GHz

Hum, Temp, and INT	R [m]	P_{Out_0} [W]	P_{Out_L} [1ft and 2ft]
74, 86, 0	2.286	-42.5	-40.8, -41.56
—	4.572	-48.8	-52.7, -61.1
—	6.858	-47.8	-45.2, -46.7
—	9.144	-48.3	-48.8, -46.6
—	11.43	-47.5	-48.7, -50.7
—	13.716	-48.7	-58.8, -59.3
—	16.002	-42.5	-54.5, -47.9
—	18.288	-50.9	-44.5, -46.7
—	20.574	-42.6	-49.9, -45.5
—	22.86	-50.05	-50.2, -48.5
—	25.146	-54.8	-57.2, -63.3
—	27.432	-67.8	-54, -46.3
—	29.718	-65.3	-58.4, -61.5
—	34.29	-65.2	-64.5, -52
—	38.862	-60.8	-60.6, -59.8
—	43.434	-55.4	-55.2, -59.5
—	46.3169	-66.2	-69.7, -63.6
—	53.9369	-56.7	-51.6, -57.3

Table 2: HyperLog® experimental data describing the environment conditions of the select environment type along with several other parameters such as, linear and lateral distance away from transmission

came nearer and nearer, until it was equal to the frequency of the radio station. The higher the power was on the oscillator, the larger the value was for the skirt width, which in turn made it so that the signal from the oscillator interfered with the radio signal on farther and farther adjacent frequencies, eventually blocking it out altogether when close enough.

4.3. Radiation Pattern

The goal here is to accurately measure an antenna's radiation pattern in 5G bands to better understand the signal's physical behavior. In order to measure an antenna's radiation pattern, you must test it in a heavily controlled environment, which is why we plan to use a vector network analyzer in an an-echoic chamber. In order to do so, the GUI that will control the antenna probe signal and the movement of the different motors on the BiSlide must be finished. This will allow us to automate and expedite a process that by hand would take weeks, perhaps months. This would fall under future plans.

5. Conclusion

Path loss in millimeter-wave vs microwave 5G bands has a marked difference. At the higher/millimeter-wave frequencies, path loss appears to be greater than in the lower, sub 5GHz and sub 3GHz frequencies. Moreover, the noise floor at the higher frequencies appears to be lower, so it would be reasonable to conclude that at the higher frequencies there is less interference/noise. This was also the case when operating the SDR at AM and FM frequencies. When the machine is tuned to the higher frequencies, well past the 88MHz to 108MHz range

Hyperlog® Angular Data at 1.9 GHz

-30°	30°	-60°	60°
-35.5	-34.8	-49.1	-45.5
-42.3	-43.3	-47.7	-53
-45.6	-52	-54.9	-52.4
-52.3	-46.8	-52.9	-50.6
-51.6	-52.5	-53.3	-58.8
-54.1	-55.8	-58.8	-78.5
-47.2	-56.1	-54.5	-52.5
-44.9	-44.2	-49.5	-50.8
-57	-54.2	-61.7	-59.8
-45	-40.1	-51.8	-50.5
-54	-60.5	-59.7	-60.4
-45.2	-43.7	-63	-49.5
-50.7	-48.5	-57.8	-52.9
-48.5	-50.5	-60.6	-55.1
-47.8	-47.4	-59.8	-52.7
-45.4	-48	-54.5	-55.9
-52.2	-55.2	-65.3	-65.3
-52.7	-51.9	-67.7	-57.6

Table 3: HyperLog® experimental data describing the environment conditions of the select environment type along with several other parameters such as, angular distance away from receiver

where FM stations operate, one could visibly observe the noise floor progressively getting lower, which further supports said conclusion. Further on it is required to measure antenna radiation patterns at 5G bands, so that the physical behavior of the signals can be better described and modeled, which in turn can provide valuable information with regards to improving and optimizing 5G signals that contain information, and improving wireless mobile communications.

6. Future Work

6.1. Phase 1: Antenna Analysis

During the in-field experiments in phase one both researchers used a tape measure of 25 ft to ascertain the appropriate amounts of distances between the receiving and transmitting antennas to deduct things such as signal threshold. Despite this knowledge the methods of such controls in ENV1 and ENV2 could have been more accurately ascertainable if measurements were done with things such as an automated measurement system. Both researchers during the phase one experiments could have used levelers to combat the possibility of the terrain of both environments being uneven. Furthermore, a tertiary environment should have been considered were the sets of in-field data lay completely open with extreme airway exposure in a public pathway.

6.2. Phase 2: SDR Studies

The SDR in-lab observations were concisely done using an omnidirectional whip antenna to servile FM stations across higher laid frequencies. What the omnidirectional whip antenna

did not do is reach smaller frequencies in the FM range which could have provided observations insight into how interference behaves at lower frequencies. Things like inductors and more omnidirectional whip antennas could have made this possible due to the fact that the whip antenna could only servile so many frequency values using the SDR software.

6.3. Phase 3: GUI Construction

Construction of GUI did not provide any data as intended because of the constraints of time both researchers faced during the actual alignment of the Bi-slides the initial days of working in the anechoic chamber. This meaning that the graphical interface provided thought the viewable git-hub server is viably unfinished due to these constraints. Further improvement to the interface can be done to make the options more user-friendly such as helpful description and allocation of objects within the options in the main menu provided in the GUI.

Acknowledgements

This work was supported in part by the NSF Center for Advanced Radio Sciences and Engineering, under Cooperative Agreement Award AST-2132229.

6.4. Personal Note

I would like to precis this when I say I would like to thank my parents, my family, and most of all the mentors that provided me guidance on this journey. It was with these people they helped provide insight into the person I wish to become. So, to them, to the people in the lab working each day towards the success that we all wish to find one day, thank you... for the memories I will cherish the rest of my life; and the knowledge I will use to cultivate to be the woman I wish to become.

References

Appendix A. Experimental Data Mentions (tables and Graphs): Phase 1

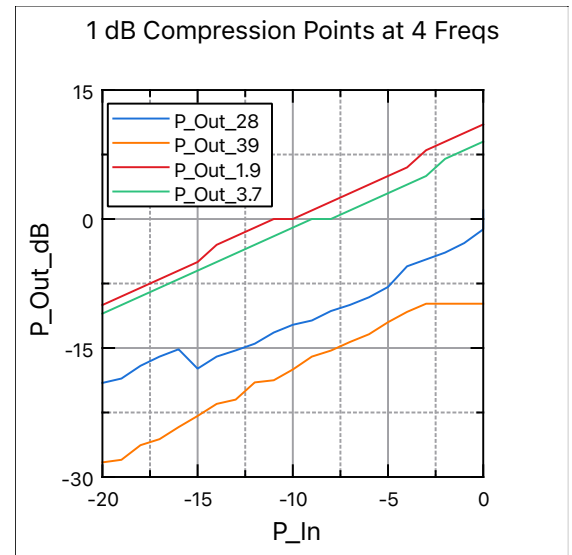


Figure A.4: A graphical representation of 1 dB compression points across all four valued frequencies

1dB compression point at 4 Freqs				
PIn	POut ₁ [28GHz]	POut ₂ [39GHz]	POut ₃ [1.9GHz]	POut ₄ [3.7GHz]
-20	-19.06	-28.3	-10	-11
-19	-18.55	-28	-9	-10
-18	-17.07	-26.3	-8	-9
-17	-16	-25.6	-7	-8
-16	-15.15	-24.2	-6	-7
-15	-17.4	-22.9	-5	-6
-14	-16	-21.5	-3	-5
-13	-15.28	-21	-2	-4
-12	-14.5	-19	-1	-3
-11	-13.2	-18.75	0	-2
-10	-12.3	-17.5	0	-1
-9	-11.8	-16	1	0
-8	-10.7	-15.3	2	0
-7	-9.99	-14.3	3	1
-6	-9.1	-13.4	4	2
-5	-7.9	-12	5	3
-4	-5.5	-10.8	6	4
-3	-4.7	-9.85	8	5
-2	-3.9	-9.85	9	7
-1	-2.8	-9.85	10	8
0	-1.2	-9.85	11	9
1	0.33	-9.85	11	9
2	1	-9.85	-11	9

Table A.4: Experimental data describing the power inputs that were put into to the Signal generator along with all of the output values across all four experimental frequency value

Gain Horn Antenna PTP Data at 28 GHz

Hum, Temp, and INT	R [m]	P_{Out} [W]
70, 86.9, 2	0.6096	-3.8
—	1.2192	-9.3
—	1.8288	-13.4
—	2.4384	-16.9
—	3.048	-19.7
—	3.3528	-19.14
—	3.6576	-20.03
—	3.9624	-19.3
—	4.2672	-20.2
—	4.572	-20.5
—	4.8768	-20.94
—	5.1816	-20.6
—	5.4864	-20.2
—	5.7912	-23.5

Table A.5: Gain Horn experimental data describing the environment conditions of the select environment type along with several other parameters such as, linear distance away from transmission

Gain Horn Antenna PTP Data at 39 GHz

Hum, Temp, and INT	R [m]	P_{Out} [W]
70, 86.9, -3	0.6096	-8.7
—	1.2192	-13.5
—	1.8288	-18.3
—	2.4384	-22.6
—	3.048	-25.7
—	3.3528	-24.6
—	3.6576	-24.7
—	3.9624	-22.8
—	4.2672	-23.7
—	4.572	-25.3
—	4.8768	-24.5
—	5.1816	-25.8
—	5.4864	-27.6
—	5.7912	-25.8

Table A.6: Gain Horn experimental data describing the environment conditions of the select environment type along with several other parameters such as, linear distance away from transmission

Gain Horn PTPL Data at 28 GHz

Hum, Temp, and INT	R [m]	P_{Out_0} [W]	P_{Out_L} [1ft, 2ft and 3ft]
79, 82.4, 2	3.048	-19.5	-22.5, -30.2, -48.8
—	6.096	-29.45	-26.3, -30.8, -37.8
—	9.144	-34.4	-32.6, -35, -30.2
—	13.716	-38.3	-34.5, -32.4, -34.3
—	18.288	-42.2	-40.8, -43.7, -42.6
—	24.284	-34.23	-40.3, -35.25, -37
—	30.48	-36.3	-41.2, -37.6, -40.2

Table A.7: Gain Horn experimental data describing the environment conditions of the select environment type along with several other parameters such as, linear and lateral distance away from transmission

Gain Horn PTPL Data at 39 GHz

Hum, Temp, and INT	R [m]	P_{Out_0} [W]	P_{Out_L} [1ft, 2ft and 3ft]
79, 82.4, -3	3.048	-26.5	-30.5, -44.2, -64.2
—	6.096	-33.5	-32.8, -40.3, -48.5
—	9.144	-39.2	-40.7, -40.5, -37.45
—	13.716	-41.5	-41.2, -40.2, -39.8
—	18.288	-49.7	-46.8, -46.7, -46.3
—	24.284	-52.6	-53.5, -52.3, -53.5
—	30.48	-49.8	-44.5, -49.2, -48.6

Table A.8: Gain Horn experimental data describing the environment conditions of the select environment type along with several other parameters such as, linear and lateral distance away from transmission

Hyperlog® PTPLA Data at 1.9 GHz

Hum, Temp, and INT	R [m]	P_{Out_0} [W]	P_{Out_L} [1ft and 2ft]
74, 86, 0	2.286	-35.4	-32.78, -33.32
—	4.572	-39.7	-37.6, -39
—	6.858	-44.6	-44.1, -39.4
—	9.144	-45.1	-35.7, -39.8
—	11.43	-45.3	-51.9, -48.7
—	13.716	-56	-47.5, -40.3
—	16.002	-47.15	-50.5, -40.5
—	18.288	-42.5	-40.8, -40.5
—	20.574	-50.4	-44.6, -41.4
—	22.86	-40.1	-38.4, -42.4
—	25.146	-54.9	-56.9, -53.5
—	27.432	-40.9	-41.9, -46.5
—	29.718	-44.1	-42.9, -46.5
—	34.29	-44.95	-54.3, -46.5
—	38.862	-44.1	-42.4, -39.9
—	43.434	-43.7	-42.9, -41
—	46.3169	-51.5	-49.6, -51.2
—	53.9369	-45.7	-45.8, -47.9

Table A.9: HyperLog® experimental data describing the environment conditions of the select environment type along with several other parameters such as, linear and lateral distance away from transmission

Hyperlog® Angular Data at 1.9 GHz

-30°	30°	-60°	60°
-35.5	-34.8	-49.1	-45.5
-42.3	-43.3	-47.7	-53
-45.6	-52	-54.9	-52.4
-52.3	-46.8	-52.9	-50.6
-51.6	-52.5	-53.3	-58.8
-54.1	-55.8	-58.8	-78.5
-47.2	-56.1	-54.5	-52.5
-44.9	-44.2	-49.5	-50.8
-57	-54.2	-61.7	-59.8
-45	-40.1	-51.8	-50.5
-54	-60.5	-59.7	-60.4
-45.2	-43.7	-63	-49.5
-50.7	-48.5	-57.8	-52.9
-48.5	-50.5	-60.6	-55.1
-47.8	-47.4	-59.8	-52.7
-45.4	-48	-54.5	-55.9
-52.2	-55.2	-65.3	-65.3
-52.7	-51.9	-67.7	-57.6

Table A.10: HyperLog® experimental data describing the environment conditions of the select environment type along with several other parameters such as, angular distance away from receiver

Hyperlog® Angular Data at 3.7 GHz

-30°	30°	-60°	60°
-44.4	-45.5	-50.5	-50
-52.4	-60.1	-58.6	-70
-47.4	-61.5	-57.5	-60
-48.5	-57.3	-55	-62.7
-49.3	-61.4	-56.1	-68.6
-57.4	-60.6	-62.6	-76.8
-51.4	-59.5	-64.7	-70.2
-51.8	48.5	-57	-60.5
-50.7	-56.4	-53.5	-63.7
-52.7	-51.25	-57.4	-72.1
-56.5	-67	-69.4	-79.1
-63.05	-80	-63.7	-88.5
-72.1	-77.9	-74.5	-85.5
-70.2	-70	-86.5	-72.2
-65.8	-74	-73.9	-75.5
-57.2	-65.3	-59.9	-78.7
-63.5	-70	-77.6	-75
-58.9	-63.6	-75.3	-67

Table A.11: HyperLog® experimental data describing the environment conditions of the select environment type along with several other parameters such as, angular distance away from receiver

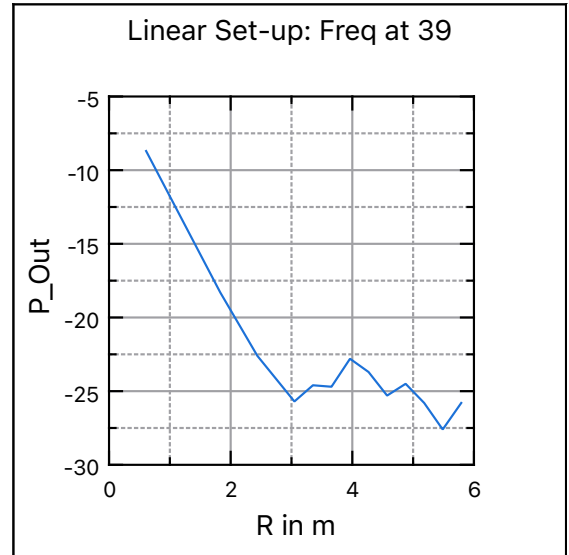


Figure A.5: A linear graphical representation of the power output as the distance increase the farther the researcher gets from the transmitting signal

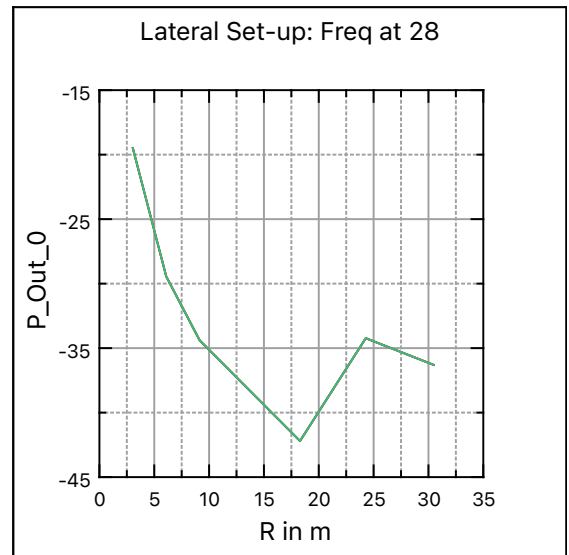


Figure A.6: A linear graphical representation of the power output as the distance increase the farther the researcher gets from the transmitting signal

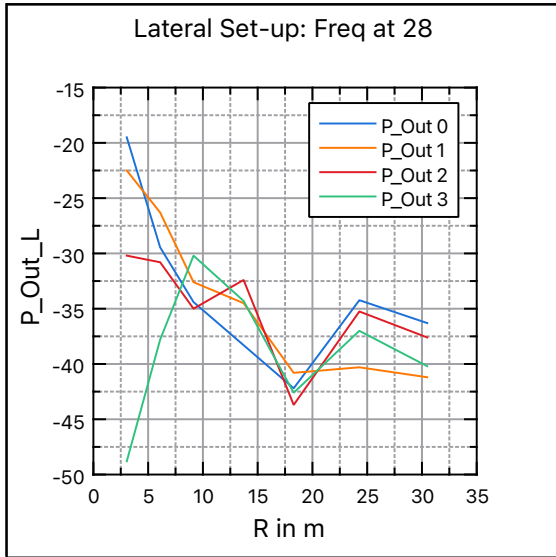


Figure A.7: A graphical representation of the lateral outputs using a Gain Horn antenna. The further the researcher got linearly across the environment the more the power outputs change in a scattered positive and negative formation.

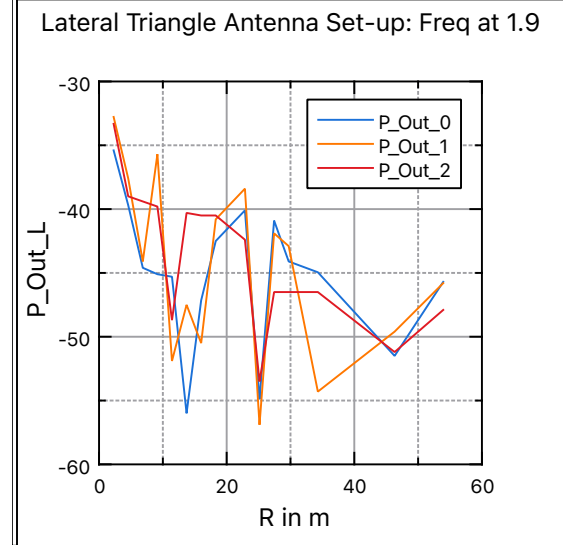


Figure A.9: A graphical representation of the lateral outputs using a Gain Horn antenna. The further the researcher got linearly across the environment the more the power outputs change in a scattered positive and negative formation.

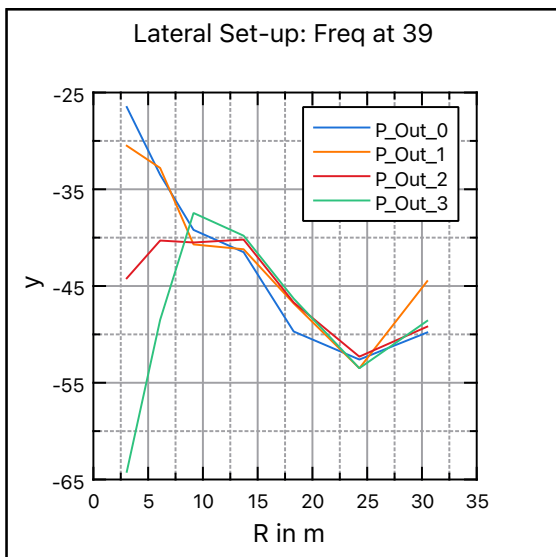


Figure A.8: A graphical representation of the lateral outputs using a Gain Horn antenna. The further the researcher got linearly across the environment the more the power outputs change in a scattered positive and negative formation.

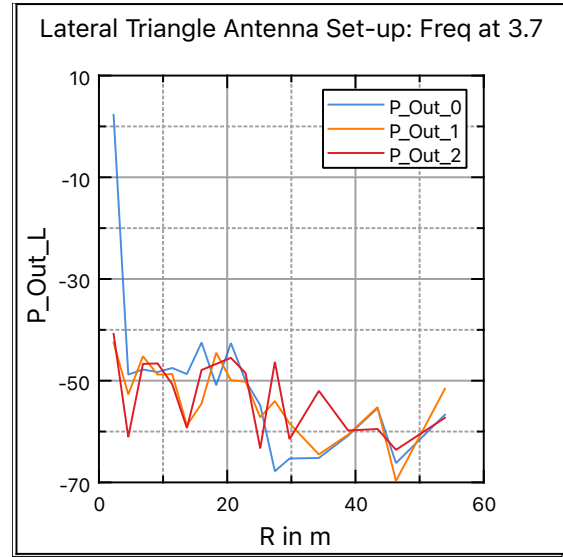


Figure A.10: A graphical representation of the lateral outputs using a HyperLog® antenna. The further the researcher got linearly across the environment the more the power outputs change in a scattered positive and negative formation.

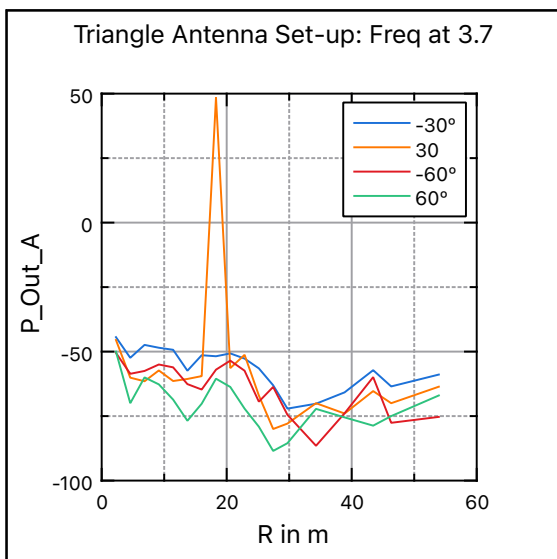


Figure A.11: A graphical representation of the lateral outputs using a Hyper-Log® antenna. The further the researcher got linearly across the environment the more the power outputs change in a scattered positive and negative formation.